On the interactions of mineral dust, sea-salt particles, and clouds: A measurement and modeling study from the Mediterranean Israeli Dust Experiment campaign

Z. Levin, A. Teller, and E. Ganor
Department of Geophysics and Planetary Sciences, Tel Aviv University, Tel Aviv, Israel

Y. Yin
Institute of Mathematical and Physical Sciences, University of Wales Aberystwyth, Aberystwyth, UK

Received 27 January 2005; revised 5 April 2005; accepted 19 July 2005; published 22 October 2005.

[1] The size distribution and chemical composition of aerosol particles during a dust storm in the eastern Mediterranean are analyzed. The data were obtained from airborne measurements during the Mediterranean Israeli Dust Experiment (MEIDEX). The dust storm passed over the Mediterranean Sea and extended up to an altitude of about 2.5 km. The uniqueness of this dust storm is that approximately 35% of the coarse particles up to about 1 km in height were internally mixtures of mineral dust and sea salt. Just north of the dust storm, large convective clouds developed, and heavy rain was recorded by the radar on the Tropical Rainfall Measuring Mission satellite. The chemical and physical properties of the particles are used as initial conditions for conducting a sensitivity simulation study with the two-dimensional detailed spectral bin microphysical model of Tel Aviv University. The simulations show that ignoring the ice-nucleating ability of the mineral dust, but allowing the soluble component of the mixed aerosols to act as efficient giant cloud condensation nuclei (CCN), enhances the development of the warm rain process in continental clouds. In our simulations the rain amounts increased by as much as 37% compared to the case without giant CCN. Introducing similar coarse-mode particles into more maritime-type clouds does not have significant effect on the cloud or on the amount of rainfall. On the other hand, allowing the mineral dust particles to also act as efficient ice nuclei (IN) reduces the amount of rain on the ground compared to the case when they are inactive. The simulations also reveal that under the same profiles of meteorological parameters, maritime clouds develop precipitation earlier and reach lower altitudes than continental clouds. When the dust particles are active as both giant CCN and effective IN, the continental clouds become wider, while the effects on the more maritime clouds is very small.

Citation: Levin, Z., A. Teller, E. Ganor, and Y. Yin (2005), On the interactions of mineral dust, sea-salt particles, and clouds: A measurement and modeling study from the Mediterranean Israeli Dust Experiment campaign, *J. Geophys. Res.*, *110*, D20202, doi:10.1029/2005JD005810.

1. Introduction

[2] The effects of aerosols on rainfall amounts are among the most uncertain factors in the role of aerosols in climate change. The complex interactions between particles and clouds depend on the particles' characteristics (concentrations, size distributions, and chemical compositions) and on the type of clouds that are involved (continental or maritime, convective or stratiform, cold or warm). Aerosols, on which cloud droplets form, determine the initial concentrations and sizes of the droplets; they influence the effectiveness of precipitation production, the scavenging efficiency of atmospheric aerosols and affect cloud's radiative properties. In addition, the clouds affect the aerosols by various chemical reactions that take place in the drops. Upon evaporation of the clouds, aerosols of different compositions are released back into the atmosphere [*Levin et al.*, 1996; *Wurzler et al.*, 2000; *Yin et al.*, 2002].

[3] Together with sea salt, mineral dust is one of the major sources of natural coarse-mode aerosols in the world [*Kouimtzis and Samara*, 1995]. Recently, using satellite observations and in situ measurements *Rosenfeld et al.* [2001] found evidence that desert dust might suppress precipitation. In contrast, *Yin et al.* [2002] and *Wurzler et al.* [2000] used numerical models to show that giant cloud condensation nuclei (GCCN) including dust coated with soluble material (e.g., sulfate) may actually increase the amount of precipitation in some clouds because of the effective growth of the drops by collection. *Yin et al.*

0148-0227/05/2005JD005810$09.00

[2002] used a 2-D model of a mixed phase cloud with detailed microphysics to show that insoluble mineral dust can become effective CCN after passing through a convective cloud. These giant CCN have a positive effect on the amount of rain in continental clouds and an insignificant effect and maybe a slight negative effect in maritime clouds. Recent measurements during the ACE-Asia experiment [*Trochkine et al.*, 2003] also showed that the chemical composition of mineral dust aerosols changed during long-range transport from China to Japan. During their transport, some of the insoluble dust aerosols were coated with sea salt and sulfate. These interactions caused the aerosols to be more soluble and increased their chance to serve as CCN. A recent study by *van den Heever et al.* [2005], who used a three-dimensional model, RAMS, to study the effects of Saharan dust (used as enhanced CCN, GCCN and IN) on Florida storms, suggested that rainfall was enhanced by dust ingestion during the first 2 hours of the formation of deep convective cells but it was reduced on the ground at the end of the day. The decrease of precipitation at the end of the day was due to the scavenging of the dust particles by the falling precipitation during the early stages of the storm.

[4] A few attempts were carried out recently, to quantify empirically how aerosol properties such as their concentrations and types affect cloud properties and precipitation. *Givati and Rosenfeld* [2004] have shown that the increase in aerosol concentrations due to air pollution in the urban areas along the eastern Mediterranean and southern California coastlines results in reduced rainfall amounts downwind of the pollution centers. They suggested that this suppression is due to a decrease in coalescence and riming resulting in a delay of rain formation. Analyses made by *Mahowald and Kiehl* [2003] have shown a relationship between thin cloud properties and mineral dust concentrations over North Africa and the north Atlantic. Like *Rosenfeld et al.* [2001] they suggested that high concentrations of mineral dust aerosols may suppress precipitation. *Borys et al.* [2003] found that enhancement in anthropogenic aerosol concentrations causes a slowdown in snow particles riming and therefore lower precipitation rate in cold clouds. Furthermore, recent simulation by *Khain and Pokrovsky* [2004] suggested that in deep continental convective clouds, the enhanced CCN could lead to increase in latent heat release and to its distribution over a larger vertical extend of the cloud, leading to taller clouds.

[5] In spite of the results mentioned above there is still a great deal of uncertainty about the role of aerosols in modifying clouds and precipitation. The eastern Mediterranean is an excellent natural laboratory for studying the interactions between clouds and aerosols because this region is affected by air masses from different sources containing anthropogenic pollution from eastern and western Europe [*Luria et al.*, 1996; *Wanger et al.*, 2000; *Andreae et al.*, 2002], marine aerosols [*Al-Momani et al.*, 1995], mineral dust particles from the North African deserts [*Ganor and Mamane*, 1982; *Levin et al.*, 1996; *Ganor and Foner*, 1996; *Mihalopoulos et al.*, 1997; *Falkovich et al.*, 2001] and biogenic material from various land and marine sources [*Ganor et al.*, 2000; *Kubilay et al.*, 2002].

[6] The eastern Mediterranean region is strongly affected by mineral dust transported from the Sahara desert. *Ganor* [1994] found an average of 19 episodes of dust per year based on 33 years of observations. Measurements by *Levin and Lindberg* [1979] showed that mineral dust aerosols are almost always present in the atmosphere in this region. Similarly by using the TOMS data *Israelevich et al.* [2003] showed that dust particles are always present, over the dust source regions in Africa, waiting for the winds to carry them to the Mediterranean or to the Atlantic regions. *Alpert and Ganor* [1993] analyzed the dynamics of a severe dust storm over the western Mediterranean region and found that it had a synoptic link with a cold front and heavy rainfall in that region. In spite of these studies, relatively few papers have appeared that discuss the properties of the mineral dust particles as a function of height. *di Sarra et al.* [2001] showed an example for measurements of aerosol vertical distribution using LIDAR in the island of Lampedusa. This study showed large aerosol concentration up to 7–8 km height when the air masses were transported from North Africa. Aerosol loading was much lower when the air masses were transported from the European continent.

[7] MEIDEX, the Mediterranean Israeli Dust Experiment was designed to investigate the vertical characteristics of mineral dust in the Mediterranean region. The campaign was carried out between 16 January and 1 February 2003 and was designed to measure dust spatial and temporal distributions by remote sensing from the shuttle Columbia in its STS-107 flight, and by simultaneous in situ measurements from a King Air airplane and from the ground. A detailed description on the project is available at http://luna.tau.ac.il/~peter/MEIDEX/home.htm.

[8] Unfortunately, the space shuttle flight ended in disaster when the shuttle and the crew were lost upon reentry into the atmosphere. Although some of the data were transmitted to ground and some was recovered after the accident, the space shuttle data from the dust storm reported here was lost. Therefore here we only discuss results from airborne measurements that were performed during the research flight of 28 January when the eastern Mediterranean region was affected by a Saharan dust storm.

[9] Our objective was to measure the vertical profiles of the chemical and physical properties of the mineral dust particles during their transport over the sea and to evaluate the potential effects they may have on cloud and rain formation in this region. While flying at different heights, we measured the particles' sizes and concentrations and sampled them for chemical analysis.

[10] These data together with typical temperature and humidity profiles for this region and for this season were used as initial conditions to simulate cloud development in our Tel Aviv University two-dimensional (TAU-2D) numerical cloud model [*Yin et al.*, 2000]. Our aim in these simulations was, among others, to evaluate the distinct influence of mineral dust, sea-salt aerosols and their mixture on precipitation development and rain amounts.

2. Measurements and Instrumentation

[11] On 27–28 January 2003 a dust storm that originated in western Africa passed over the southeastern corner of the Mediterranean Sea.

[12] A meteorological analysis that was carried out for that period shows that a cold cyclone passed over the

eastern Mediterranean Sea. The cyclone moved slowly from Crete through Cyprus toward Iskenderun bay (Turkey). This cyclone was accompanied by a cold front that moved eastward toward the Israeli coastline. The front was located between Antalya (Turkey) and the northern Sahara Desert (between Egypt and Libya) and passed over the sea. The northern part of the Mediterranean Sea was influenced by strong northwesterly wind with vertical convections and turbulence. In the regions to the south over the sea and over the desert the winds were southwesterly with velocity of 8–10 m s^{-1}. These latter winds formed a dust layer up to an altitude of about 2500 m above mean sea level (msl). The dust was accompanied by a haze layer and nonprecipitating cumulus clouds. At the region where these two air masses met, deep convection was developed, as can be seen from the Moderate Resolution Imaging Spectroradiometer (MODIS)-Aqua images at 1100 UT on this day (Figure 1). At about the same time the Tropical Rainfall Measuring Mission (TRMM) satellite passed over the region and its radar recorded about 10–20 mm h^{-1} in region A and heavier precipitation (30–50 mm h^{-1}) in the cloud clusters marked as B and C in Figure 1. The clouds in these clusters reached high altitudes with temperatures lower than −30°C, as obtained from the MODIS data. Large anvil with ice can be seen in cluster B in Figure 1, which is in agreement with the analysis of the cloud product from MODIS. PM-10 measurements made by the Israeli Ministry of Environment near the ground in Tel Aviv on 28 January revealed a dust concentration of 657 μg m^{-3} while normally the PM10 load at the same place is about 50 μg m^{-3}. The dust was dispersed by the strong wind over central and southern Israel on 29 January, with hail and heavy rain amounts (50–60 mm), causing some flooding and damage to agriculture, as recorded in the northern regions of Israel by the Israeli Meteorological Service.

[13] On the morning of 28 January a research flight was conducted at about 20–100 km from the southeast coast of the Mediterranean Sea. The flight area and time period were planned in order to perform simultaneous measurements with the observations by the space shuttle Columbia that passed overhead. Aerosol sampling started only after the plane reached above the dust storm in order to prevent contamination of the sampling tube and in order to reach the proper altitude for the simultaneous measurement with the shuttle.

[14] Figure 1 shows the flight track in the measurement area projected on the MODIS-Aqua image that was taken on 28 January at 1100 UTC. A back trajectory analysis for the measurement period was carried out using the NOAA Hybrid Single Particle Lagrangian Integrated Trajectory (HYSPLIT) model (http://www.arl.noaa.gov/ready/hysplit4.html). The back trajectories of the wind flow directions (not shown here) reveal that the dust storm originated from the northern regions of Libya and Egypt in agreement with the MODIS image.

[15] Our airborne measurements were carried out on board a King-Air airplane (Beechcraft C-90). The airplane was equipped with various instruments for measuring aerosols number concentrations and size distributions in the range 0.11–32 μm and to sample aerosols on filters and on electron microscope grids. In addition, temperature sensors, GPS and white light albedo meter (not analyzed in this paper) were also mounted on the airplane.

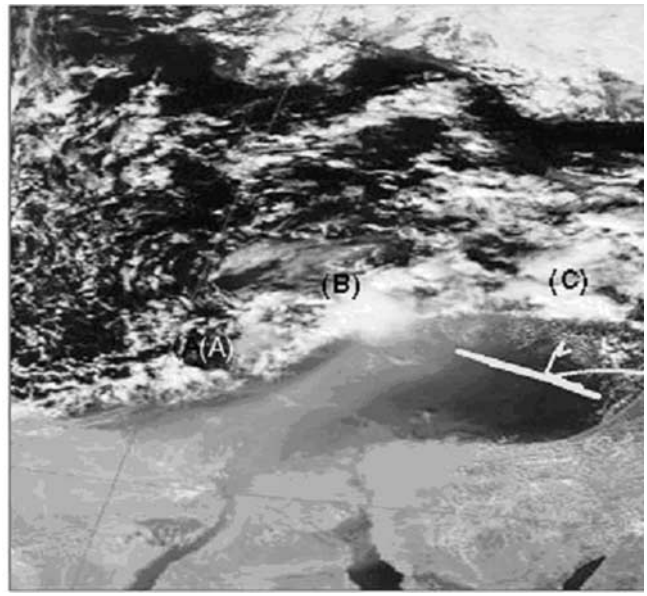

Figure 1. Moderate Resolution Imaging Spectroradiometer (MODIS)-Aqua image of the dust storm on 28 January 2003. The white line represents the track of the research airplane. The airplane carried out measurements at different altitudes along the marked line. The regions marked as (A), (B), and (C) represent cloud clusters with different types of clouds and different amounts of precipitation as seen by Tropical Rainfall Measuring Mission (TRMM) radar; see text for discussion.

[16] Aerosol size distributions and concentrations were measured using two optical particle counters (OPC): a Droplet Measurements Technology (DMT) SPP-200 (a modified PMS-PCASP-100) for aerosols in the range 0.1–3 μm equivalent optical diameter (EOD), and a DMT SPP-100 (a modified PMS-FSSP-100) for aerosols in the range 2–16 μm EOD. During periods when the airplane measured cloud properties the SPP-100 was set to measure aerosols and cloud droplets in the range 3–32 μm EOD.

[17] Both instruments were calibrated before the campaign with glass beads (for the SPP-100) and polystyrene latex (PSL) particles (for the SPP-200) of known diameters. The aerosols were binned into 30 diameter intervals for calculating their size distribution. In both instruments the first bin was excluded from the analysis because of possible noise contamination. Data collected from the SPP-200 and the SPP-100 were combined for presentation on the same graph by averaging the overlapped measurements of both instruments in the range 2–3 μm. In order to keep a constant airflow at the instruments inlet, a constant airplane speed of 70 m s^{-1} was maintained during the measurements periods.

[18] Sampling of aerosols on board the airplane was carried out using two systems that were designed and built in the Laboratory of Cloud and Precipitation in TAU. One system used a single stage impactor, which was placed in the airplane as part of a specially designed sampling system (Figure 2a). The second system consists of a sampling instrument, called a Big Particle Sampler (BPS), which was mounted on top of the airplane fuselage on a specially designed pedestal, 50 cm high, in order to collect particles larger than 2 μm (Figure 2b).

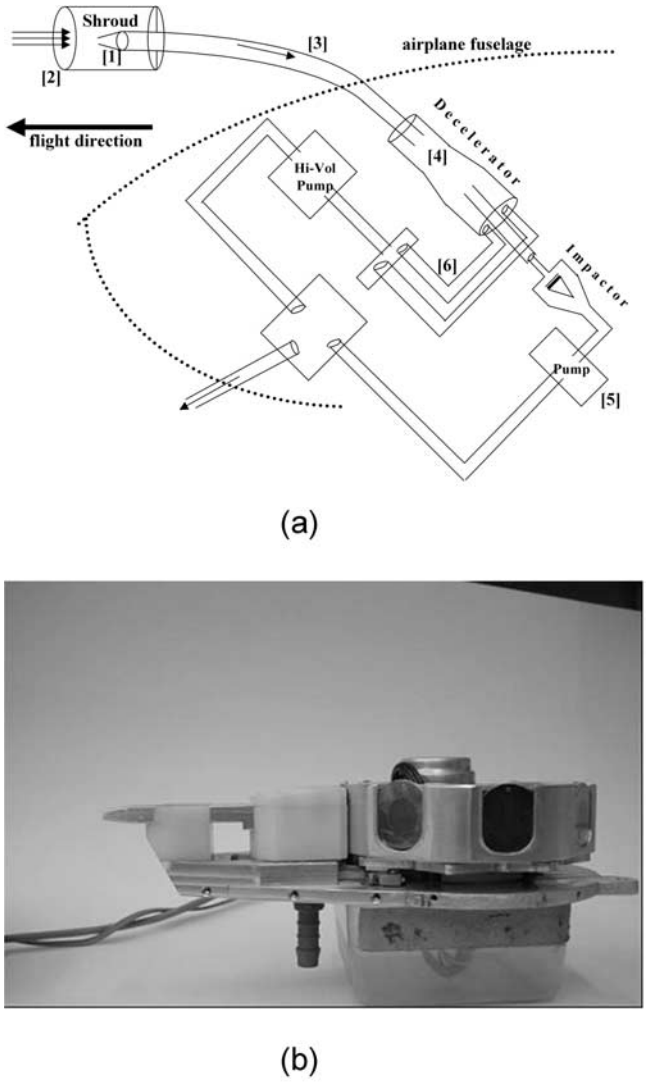

Figure 2. (a) General structure of the King-Air internal sampling system. (b) Picture of the Big Particle Sampler.

[19] The size and the diameters of the tubes in the sampling system were designed to provide isokinetic flow from the outside into the airplane [*Kouimtzis and Samara*, 1995] and in compliance with the flow rate requirements of the impactor.

[20] During the flight, air penetrates the sampling system through an inlet of 1.3 cm diameter ([1] in Figure 2a), which is concentrically covered by a shroud (11.5 cm diameter, 23 cm long) [2] for flow straitening prior to entering the sampling tube (2.5 cm diameter). The air decelerates from $\sim$70 m s^{-1} (the airplane speed) to $\sim$25 m s^{-1} as it passes through the small inlet [1] into the larger diameter tube [3]. In order to bring the air from the outside into the airplane and to prevent extensive losses of aerosols to the walls, the tube was bent at 130° [3]. A second decelerator in the form of a cone (8°) is mounted inside the cabin [4]. A small tube, 8 mm diameter, is placed in the middle of the cone at a location where the airflow is equivalent to a flow rate of 20 LPM, which is the required flow rate for the impactor. This sampling tube is connected to the impactor. The air speed at the location of the sampling tube was calculated on the basis of mass conservation and was checked by measurements prior to the final mounting using a small Pitot tube, which was inserted into the cone.

[21] The constant flow through the impactor is controlled by an additional pump [5]. This pump allows only a small fraction of the air ($\sim$5%) to be pumped through the impactor by passing through the narrow tube. Since the airplane is pressurized, the sampled air that passes through the tube and through the two pumps is exhausted outside the cabin through a number of discharge tubes [6].

[22] Analytical and numerical calculations of the system's aerosol collection efficiency were not carried out because the sampling system was aimed to characterize only the chemistry of the particles and not their physical properties. Comparison between the physical sizes of aerosols that were simultaneously collected by the impactor in the sampling system with a BPS sample showed a good agreement up to about 2 μm particle size. Above this size, the concentrations of the collected aerosols in the sampling system decrease slowly, so that particles larger than about 8 μm are rarely seen.

[23] The single-stage impactor was used to collect particles on electron microscope Thermanox grids. The grids were precoated with a thick layer of carbon in order to differentiate droplets from dry aerosols (in cases of high relative humidity) by identifying the ringed dark contour around the aerosol, and to identify the particles' shape and elemental composition (single particle analysis). The elemental compositions of individual particles were analyzed using a Scanning Electron Microscope (SEM) JEOL JSEM 6400 with an Energy Dispersive X-ray Spectrometer (EDS).

[24] During their impaction the particles were deposited around a narrow strip along the center of the grids. Large particles usually impacted at the center of the strip while smaller particles were diverted toward the edges. The selection of particles for EDS analysis was done by moving the detector along a cross section between the two sides of the strip and perpendicular to it. The location of the sampling cross section was selected randomly. An X-ray spectrum was integrated for 50 s for every EDS analysis.

[25] The analysis consists of finding the elemental mass of different particles by using a calibration method that had been developed by *Pardess et al.* [1992] and *Levin et al.* [1996]. With this method one could estimate the elemental mass by comparing the X-ray counts of the inspected particles with the counts of calibrated particles of known masses. For particles $d < 0.4$ μm the signals in the EDS analysis become similar to the background noise and therefore our EDS analysis is applicable only for particles $d > 0.4$ μm.

[26] The sampling system allowed most particles to be sampled inside the airplane. However, some of the big particles (larger than 2 μm) were lost to the walls of the sampling system; we therefore developed the Big Particle Sampler.

[27] The Big Particle Sampler (BPS) (Figure 2b) was designed and installed on board in order to collect large aerosols (larger than 2 μm) with high efficiency. During MEIDEX, the instrument was mounted on top of the airplane and particles were collected by impacting on similar grids to those used inside. The uniqueness of the BPS is the ability to collect particles and to change the

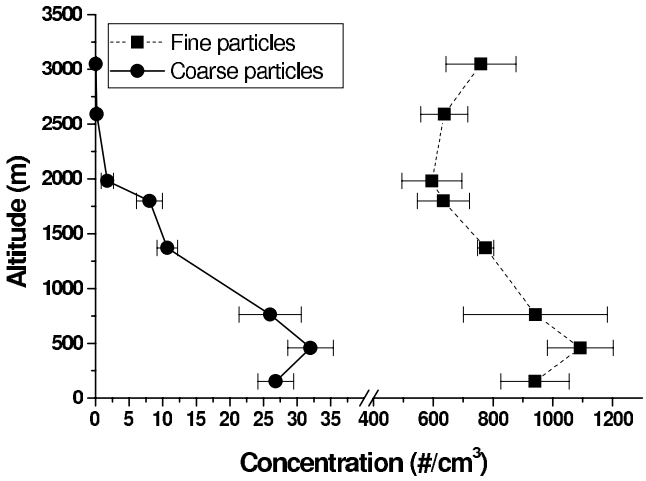

Figure 3. Vertical profile of total aerosol concentrations of fine (d < 1 μm) and coarse (d > 1 μm) aerosols and their variability during the dust storm of 28 January 2003.

collecting surface during the flight by exposing new grids into the flow. The instrument was designed to have 8 such grids, each rotated into position when needed.

[28] The determination of the sizes of the inlet and outlet holes were done using Computational Fluid Dynamics software (FLUENT) and by analytical calculations presented by *Kouimtzis and Samara* [1995]. The calculations were carried out in order to assure that only particles greater than 2 μm would impact the grids. To assure isokinetic flow inside the BPS a flow rate of about 30 L min^{-1} is needed. We set the inlet size to 2 mm width in order to assure isokinetic flow at the inlet and to have a cutoff particle size larger than 2 μm. This value was chosen to suit an airplane speed of 70 m s^{-1}.

3. Results

3.1. Aerosol Concentrations and Size Distributions

[29] Using the data from the optical instruments we calculated the aerosol concentrations and their size distributions at different altitudes. Each lag lasted at least 5 min in order to improve confidence in the results. Although the optical instruments integrated the measurements every second, we used a 10-s running average for smoothing. Figure 3 shows the average vertical profile of the fine (d < 1 μm) and coarse (d > 1 μm) aerosol concentrations.

[30] The coarse particles concentration decreased from about 30 cm^{-3} near the sea surface to about 1 cm^{-3} at an altitude of 2200 m. The fine particles followed a similar profile up to approximately 2 km but with much higher concentrations of ~1000 cm^{-3} near the surface (around 250 m) to ~600 cm^{-3} at 2000 m. However, above 2000 m the fine particle concentration increased again, probably because of the lack of larger particles on which to aggregate. These results show that the thickness of the dust layer was 2–3 km above msl.

[31] Figure 4 shows the vertical profile of the aerosol size distribution calculated from the measurements of the optical counters. Three size modes at ~0.2 μm, 0.8 μm and 2 μm were observed up to about 500 m. The fine particle concentration at 0.2 μm was ~1000 cm^{-3} μm^{-1} and remained the same up to an altitude of about 1700 m above msl. High concentrations of coarse particles of ~2 μm were found up to 2500 m. Figure 4 also shows that particles as large as 5–8 μm were found as high as 2000 m.

[32] During the flight the airplane passed through shallow cumulus clouds that were formed at the north end of the flight area, but still south of the main cloud clusters shown in Figure 1. Figures 5a and 5b show the averaged aerosol and cloud droplets size distributions and volume distributions below cloud base (averaged over 30s flight time at 70 m s^{-1}) and in cloud (averaged over 10-s flight time). Figure 5 reveals that the cloud had only a few droplets with sizes approaching 20 μm, not large enough to efficiently grow by the collision-coalescence process. The concentration of the fine aerosols fraction (d < 1 μm) that was obtained from integrating the size spectra up to 1 μm was about 950 cm^{-3}, which is similar to the measured concentrations at the same altitude within the dust. In other words, a large fraction of the fine particles did not nucleate to form droplets.

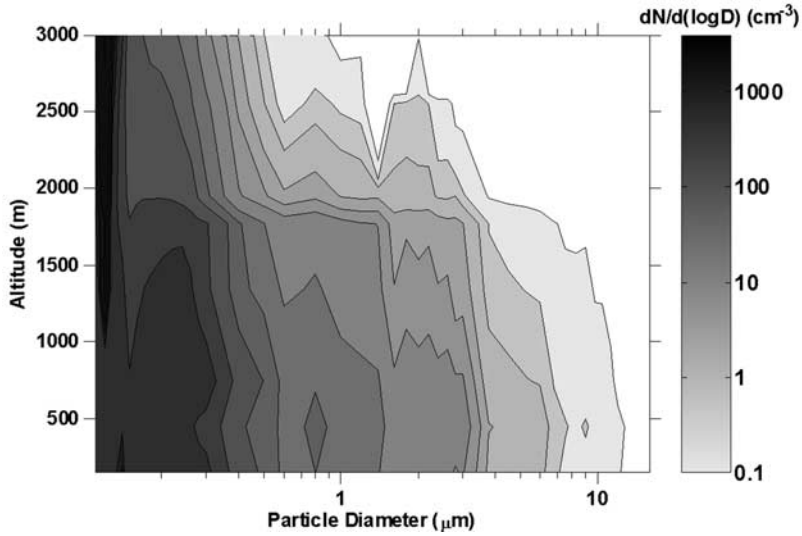

Figure 4. Vertical profile of aerosol size distribution measured by the SPP-100 and SPP-200 on 28 January 2003. The contours represent the different values of dN/dlogD.

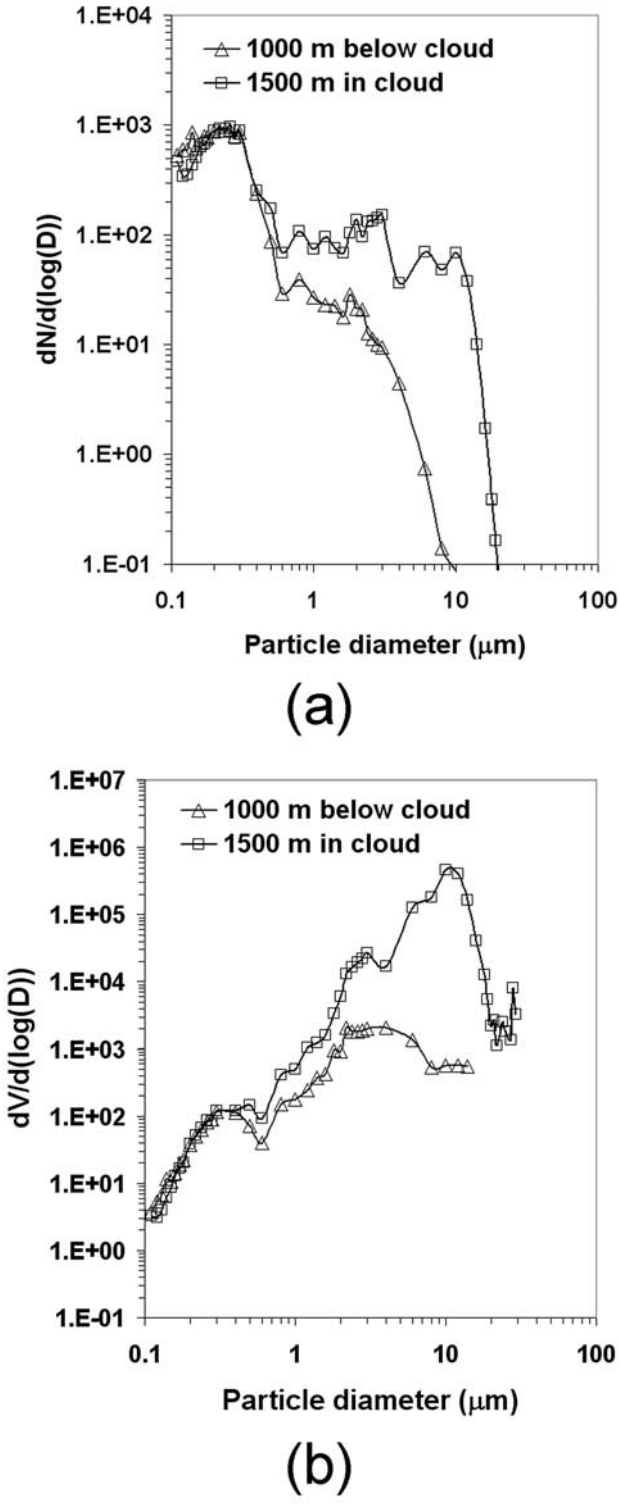

Figure 5. Aerosol and cloud droplets (a) size and (b) volume distributions below cloud base and in cloud as measured by the optical particle counters during the research flight, 28 January 2003.

[33] The coarse particle concentration just below cloud base reached about 25 cm^{-3}, which is similar to the vertical profile presented in Figure 3. Inside the cloud at a height of 1500 m (temperature of about 7°C), the concentrations of the droplets (assuming all the particles larger than 1 μm were droplets) reached a maximum value of 350 cm^{-3}. Analysis of the volume distribution profile below cloud base reveals high aerosol loading in the coarse fraction typical for an environment that contains large mass of mineral dust. It is important to note again here that the convection in the measured clouds was not strong and only shallow clouds were seen in the measuring site. Most of the drops were probably nucleated on the large soluble particles, leaving most of the fine particles inactivated. This is the reason the droplet concentration was relatively low with particles mostly smaller than 10 μm.

3.2. Chemical Analyses

[34] Samples from four altitudes (500, 1000, 1500 and 2000 m) were chosen for quantitative elemental and morphological analysis using SEM-EDS. In addition, a sample that was collected in cloud (at altitude of 1500 m) was analyzed in order to compare its chemical composition with that of the dust layer.

[35] The samples were collected on Thermanox substrate. Since Thermanox contains carbon, the present method could not identify this element. Similarly, quantitative estimation of the mass of nitrogen could not be obtained because of the proximity of its peak to that of carbon in the X-ray spectrum. In order to identify carbon and nitrogen we produced images of a few particles using the X-ray mapping feature of the EDS controlling software (Oxford Link ISIS). These images represent the particles' morphology by counting the detected X-ray signals for every element separately.

[36] The SEM-EDS was used to identify the following elements: Na, Mg, Al, Si, S, K, Cl, Ca, and Fe. The analyzed particles were divided into four groups on the basis of their chemical composition [*Ganor et al.*, 1998]: (1) sea-salt aerosols, containing sodium and chloride (NaCl), sometimes together with Mg, S, Ca and/or K; (2) air pollution particles, containing only sulfur (possibly sulfuric acid (H_2SO_4), ammonium sulfate ($(NH_4)_2SO_4$, or ammonium bisulfate (NH_3HSO_4)), only sodium (sodium nitrate ($NaNO_3$)), or Na and S (sodium-sulfate (Na_2SO_4)); (3) mineral dust particles, containing Mg, Al, Si, Ca, and Fe; and (4) sea salt plus mineral dust (mixed aerosols), containing mixtures of sea salt and mineral dust.

[37] The particles were also classified on the basis of size as fine (d < 1 μm) or coarse (d > 1 μm). Six hundred sixty particles were analyzed for their elemental composition, 230 of which were smaller than 1 μm while 430 were larger then 1 μm.

[38] Table 1 shows the fractions by number of occurrence of each group in its own size category. Each value in the table represents an average from the entire samples in each size and height category.

Table 1. Classification of Individual Particles by Fraction of Number of Occurrence

	Within Dust				In Cloud, H = 1500 m	
	H < 1000 m		H > 1000 m			
	Fine	Coarse	Fine	Coarse	Fine	Coarse
Marine	0.43	0.13	0.10	0.10	0.33	0.39
Mineral	0.39	0.47	0.50	0.34	0.67	0.38
Air pollution	0.12	0.04	0.35	0.48	0.00	0.07
Marine with mineral	0.06	0.36	0.05	0.08	0.00	0.16

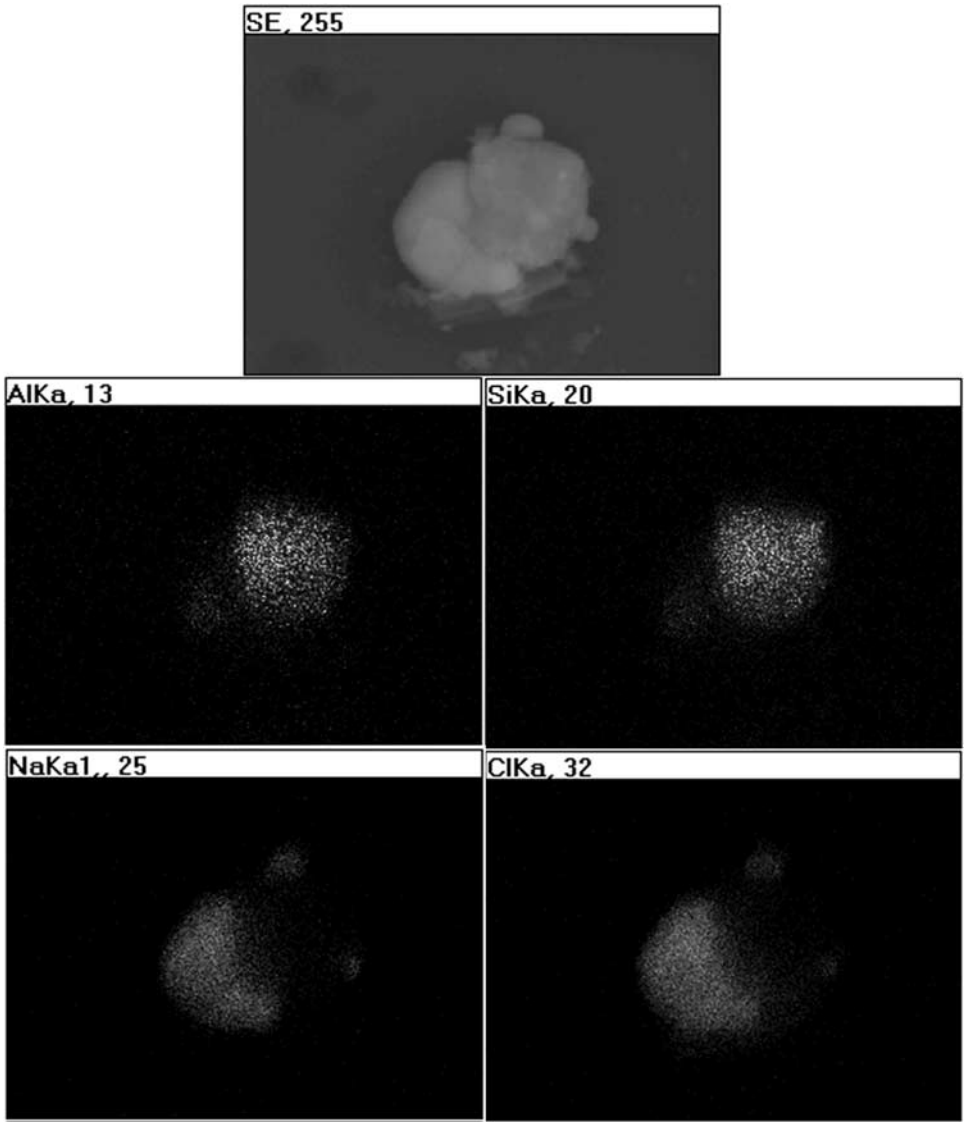

Figure 6. X-ray mapping of an aggregate with diameter of 5 μm containing sea salt (NaCl) and clay mineral (Al and Si) sampled at 500 m above mean sea level.

[39] At low altitudes of up to 1000 m above msl, which corresponds to the height of the cloud bases that appeared to the north of the main mass of the dust storm, the most prominent aerosol types were sea salt, minerals and aggregates of mineral dust and sea salt (which were mostly present in the coarse mode). The particles above 1000 m were mostly minerals and air pollution particles (sulfate and nitrates). We can therefore conclude that about one third of the aerosols that entered the cloud were sea salt (both fine and coarse) and about 36% of the coarse particles were mixtures of mineral dust and sea salt. Both of these types of particles could serve as efficient cloud condensation nuclei.

[40] The analysis therefore shows that many of the aerosols (especially in the coarse mode) were internally mixed. Since the hygroscopicity of the particles is determined by the amount of the soluble material as well as by the spatial distribution of the soluble material in the particle (imbedded or on the surface), it is important to determine the morphology and the approximate location of the soluble component.

[41] X-ray mapping of some of the particles revealed that elements were dispersed nonuniformly on them, meaning that many of the mixed particles were aggregates of NaCl with minerals or aggregates of minerals with particles from sources of air pollution. An example of internal mixing due to aggregation of clay mineral (containing Al and Si) with sea salt is illustrated in Figure 6. Figure 6 shows an X-ray mapping of a 5 μm aerosol particle collected at 500 m above msl.

[42] Since we are interested in the potential effects of the particles and especially the large ones on cloud processes, it is important to increase our confidence in the measurements of chemical composition of the coarse particles. For this purpose we analyzed for size and chemical composition a set of simultaneously collected samples at 500 m on both the impactor inside the plane and the BPS. Both samples

showed very similar compositions although fewer coarse particles were collected on the impactor in the plane. This strengthens our confidence that a large fraction of the coarse particles (>2 μm) were indeed aggregates of sea salt and mineral dust.

4. Discussion and Comparison With Cloud Microphysical Model

[43] The presence of mineral dust and especially the high percentage of mixtures of mineral dust and sea salt raise questions about the potential effects of these particles in cloud formation processes and precipitation development. As can be seen in Figure 1, large cumulus clouds developed in the region where dust and clouds met. It is probably impossible to answer in absolute terms whether it is the interaction of the two air masses or the effects of the dust particles on the cloud microphysics that is mostly responsible for the development of the large clouds and the heavy precipitation. However, it could be valuable to try to isolate these two effects and study the impact of the aerosols alone. This is the objective of the following sections in this paper.

[44] To better understand the role of dust aerosols in cloud and precipitation formation we simulated cloud development with and without the types of particles that we measured. Previous works have shown that large dust particles coated with soluble material are efficient CCN [*Levin et al.*, 1996] and that mineral dust particles are also efficient ice nuclei (IN) [e.g., *Grosch and Georgii*, 1976; *DeMott et al.*, 2003]. For this purpose we used the Tel Aviv University 2-D numerical cloud model (TAU-2D) with detailed treatment of the cloud microphysics. This model uses the Spectral Method of Moments [*Tzivion et al.*, 1987; *Reisin et al.*, 1998] for calculating the growth of water drops and ice particles by various processes such as nucleation of water and ice, condensation, collection, riming, melting, drop breakup and sedimentation. The cloud is initiated with a short pulse of temperature and humidity just below cloud base. The model is used with 300 m vertical and 300 m horizontal grid spacing.

4.1. Model Setup and Initial Conditions

[45] The initial temperature and humidity profiles for all the simulations were selected to represent average thermodynamic conditions of winter convective clouds in the eastern Mediterranean region (Figure 7). The temperatures at the sea surface and at cloud base (about 1000 m) were 19°C and 8°C respectively. The humidity profile was similar to the profile shown by *Yin et al.* [2002]. For the purpose of the comparison in this paper we only used atmospheric conditions without wind shear. A more comprehensive modeling study in which wind shear is included will be completed shortly.

[46] The initial conditions for the vertical distribution of the CCN concentrations and chemical compositions were set based on our measurements up to an altitude of 1000 m above msl. The aerosol concentration of the fine fraction was about 900 cm^{-3}, corresponding to continental-type clouds (in the modeling study, fine particles are defined as particles which are smaller than 0.5 μm in diameter). For the purpose of studying the sensitivity of the cloud to CCN concentrations below cloud base, this scenario takes into account that all these aerosols could serve as CCN. In order to assess the sensitivity of the model to CCN concentrations we used another scenario called "semicontinental" with fine mode aerosol concentration of 300 cm^{-3}. The initial aerosol concentrations in all these cases remain constant from the surface to 1 km and then decrease exponentially with height with a decay factor of 2000 m (the concentrations decreased to 1/e of their values near the surface).

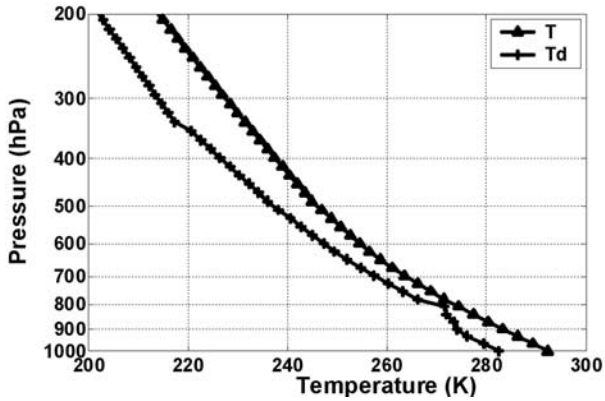

Figure 7. Temperature and dew point temperature profiles used as initial conditions in all the model simulations.

[47] Using the SEM-EDS analysis (Table 1), we evaluated the fraction (both in the fine and the coarse mode) of dust aerosols containing soluble components. These mixed aerosols are treated here as CCN because of their higher solubility. Our measurements showed that about one third of the aerosols in the coarse mode were mixed aerosols while their presence in the fine mode was very low (6% of the entire population). In our simulations below we assume that all the fine aerosols are efficient CCN, while only 33% of the observed coarse-mode particles (up to 1000 m) are efficient CCN. We also assumed that all CCN are sea salt.

[48] In the simulation runs, the particles enter the clouds and nucleate drops based on the supersaturation and critical diameter following the classical Köhler theory [*Pruppacher and Klett*, 1997]. The drops grow by condensation and then by collision-coalescence processes. As the cloud develops vertically, reaching subfreezing temperatures, ice crystals begin to form by the freezing of cloud drops containing efficient IN, primarily those containing mineral particles. Contact nucleation due to collisions of drops and IN is accounted for using the parameterization of *Meyers et al.* [1992]. Ice particles also form through ice multiplication process induced by collisions of large drops and ice particles occurring at temperatures of −4°C to −8°C [*Hallett and Mossop*, 1974]. The ice crystals grow by deposition and aggregation to form snow and by riming to form graupel particles. The large graupel particles and the large ice crystals eventually begin to descend, melting on their way down to form raindrops. Large raindrops collide with other raindrops and break up to form smaller drops based on the algorithm of *Reisin et al.* [1998] and the distribution of *Low and List* [1982a, 1982b].

[49] For the simulations in which dust was absent from the clouds, the concentration of ice crystals was parameterized on the basis of the approximation of *Meyers et al.* [1992]. This approximation considers the nucleation of ice

Table 2. Initial Conditions for the Different Scenarios Used in TAU-2D Cloud Model[a]

Case	Scenario	Concentration Fine Particles, particles cm^{-3}	Concentration Coarse Particles, particles cm^{-3}	Ice Nuclei Enhancement Factor
1	continental reference	900	0	1
2	continental with dust as IN	900	0	10
3	continental with GCCN	900	15	1
4	continental with GCCN and dust as IN	900	15	10
5	semicontinental reference	300	0	1
6	semicontinental with dust as IN	300	0	10
7	semicontinental with GCCN	300	15	1
8	semicontinental with GCCN and dust as IN	300	15	10

[a]TAU-2D stands for Tel Aviv University two-dimensional.

crystals by deposition, contact and condensation-freezing. It also states that the concentration of IN in the atmosphere is proportional to the supersaturation, when dealing with deposition or condensation-freezing processes, and proportional to the supercooling when contact nucleation is considered. However, this parameterization does not fit conditions in dust storms. There have been numerous publications showing that dust particles are efficient IN. For example, *DeMott et al.* [2003] measured the IN concentrations in a dust layer that was transported from Africa to Florida. They showed that between about 1.5 and 4 km altitude the IN concentrations at $-38°C$ were about 1 cm^{-3}. These values were about 20 to 100 times higher than those measured at lower altitudes in a nondusty environment at the same location. Note that these measurements represent all the IN that nucleate ice down to $-38°C$. In the Mediterranean clouds simulated here the clouds only reached about $-30°C$, therefore the IN concentrations would be expected to be lower. Since no IN measurements were conducted in our experiment we assumed that the concentration of IN increased by a factor of 10 above the clean background environmental values given by *Meyers et al.* [1992]. This increase is used as an illustration of the potential effects of mineral dust on clouds and it could be modified if IN measurements in dust storms in this region become available.

[50] In order to study the potential role of dust and sea-salt aerosols on cloud and rain formation, including the effect of ice nuclei concentrations, we used eight different scenarios with different size distributions and dust contribution as initial conditions. Table 2 summarizes the eight scenarios that were used in the simulations. The scenarios were characterized on the basis of the fractions of CCN (soluble aerosols) in the fine and course mode. Here we regard particles with diameter >0.5 μm as coarse-mode particles corresponding to the SEM-EDS classification that was shown in Table 1.

[51] Figure 8 shows the aerosol size distributions that were used in the eight scenarios. The CCN size distributions were not affected by the contribution of dust to ice production and therefore Figure 8 contains only four distributions (the other four scenarios in which dust aerosols contribute to IN concentrations: cases 2, 4, 6, and 8 in Table 2 had the same aerosol size distributions).

4.2. Results of Simulations

4.2.1. Effects of Giant CCN and Dust on Rain Production

[52] Figure 9 shows the amount of rain that fell from a cloud for each of the eight scenarios. It should be noted that since the model is only two-dimensional, the total amount of rain was calculated assuming that the cloud has a horizontal thickness of 1 km. The first thing that becomes clear is that the amount of rain falling from a maritime (semicontinental) cloud is much higher than from a continental cloud (compare the reference cases (cases 1 and 5 in Table 2) in Figures 9a and 9c). Furthermore, a comparison between Figures 9a and 9b reveals that the effect on continental clouds of the GCCN in the form of dust particles coated with sea salt but without their effects as IN (case 3 in Table 2), is to initiate the precipitation earlier and to increase the amount of rain on the ground by about 37% (from 7200 m^3 to 9900 m^3). In contrast, the contribution of these mixed aerosols to the development of the semicontinental case (case 7 in Table 2) is negligible and the total precipitation on the ground remains unaltered (compare Figures 9c with 9d). Similar effects in stratocumulus clouds, but with smaller increases were also reported by *Feingold et al.* [1999]. They showed that the relative impact of GCCN increases with increase in the CCN concentrations.

[53] Figure 9 also shows that, at least under the temperature profiles found in the Mediterranean region, inclusion of the effects of higher ice crystals production by dust particles (cases 2, 4, 6 and 8 in Table 2) delays the initiation of the rain and leads to a reduction of about 30% in the total rainfall amount, as compared with the case having dust and salt as only large and GCCN (Figures 9b and 9d for the continental and continental cases respectively). These results are in agreement with those of *Yin et al.* [2000].

4.2.2. Effects of Giant CCN and Dust on Clouds' Microphysical Properties

[54] In order to better understand the effects of the GCCN and the enhanced IN on the clouds it is instructive to first look at the distribution of the particles in the reference cases (cases 1 and 5 in Table 2). For these two cases Figure 10 compares the number size distribution of water drops, ice crystals and graupel particles as a function of height at 26 and 46 min at the center of the cloud. Up to about 36 min the continental cloud (not shown here) had higher droplet concentrations from cloud base to cloud top, slightly lower ice crystal concentrations and very few graupel particles with sizes of less than 0.8 mm diameter. At 46 min Figure 10 shows that the semicontinental cloud is already precipitating while only very few raindrops fall out of the continental cloud. The ice crystals in the continental clouds are located at higher levels and are found in higher concentrations. In contrast, in the semicontinental cloud the graupel particles are larger and are spatially distributed over a larger vertical extend. The graupel particles are larger because the riming process is more efficient in the presence of larger drops that

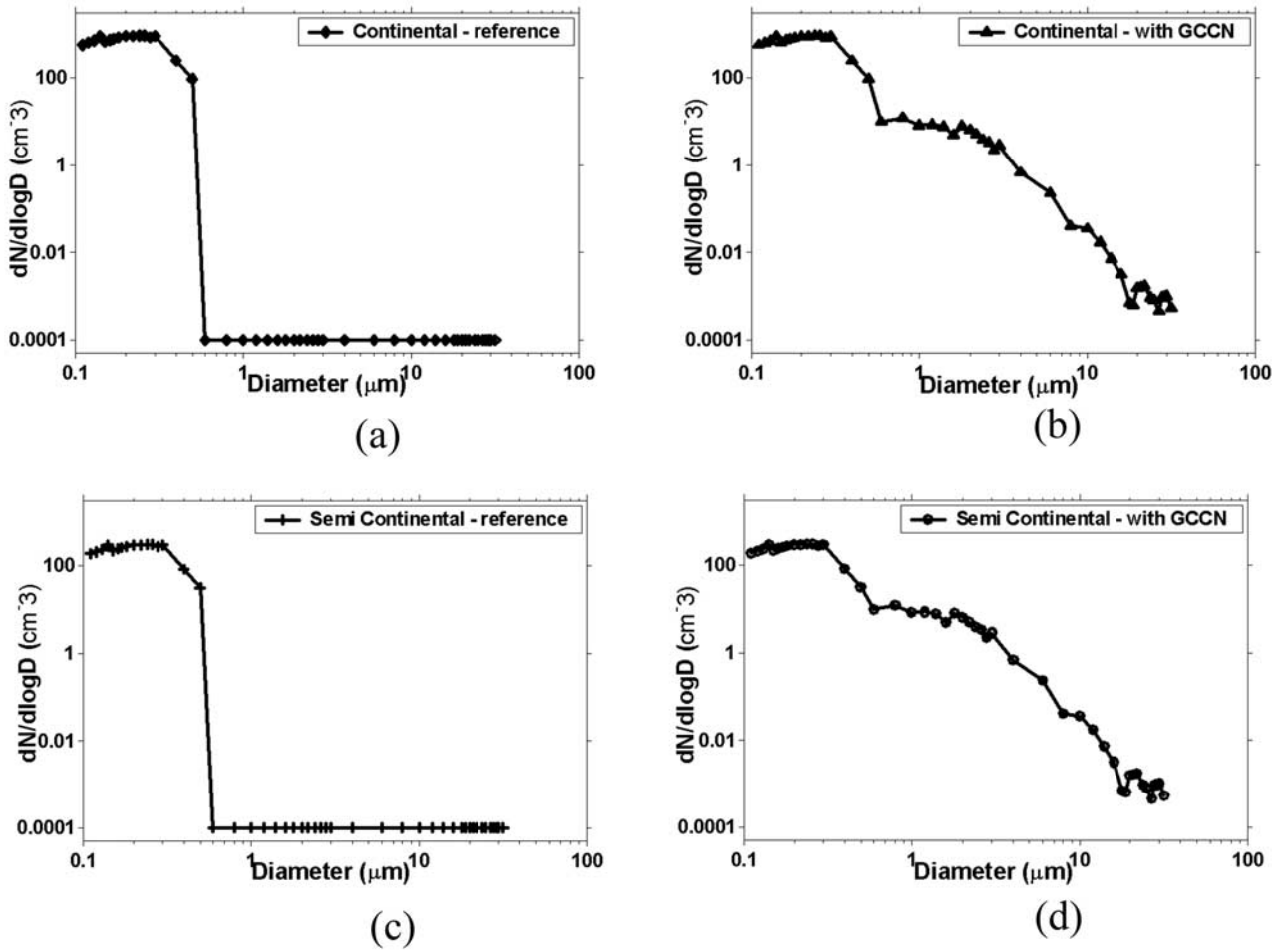

Figure 8. Initial aerosol size distributions used in Tel Aviv University two-dimensional cloud model, corresponding to the following scenarios in Table 2: (a) 1 and 2, (b) 3 and 4, (c) 5 and 6, and (d) 7 and 8.

are found in the cleaner environment represented here by the semicontinental cloud. Similar conclusions were also reached by *Borys et al.* [2003] for orographic clouds. The higher concentrations and slightly larger size of the ice crystals in the continental cloud stems from the fact that the smaller cloud drops in the continental cloud are not depleted by riming, resulting in enhanced ice crystal growth through the Bergeron-Findeisen mechanism and formation of ice particles by freezing.

[55] Some of the water seen below cloud base (see Figures 10g and 10h) originates from melted graupel particles, as expressed in Figure 10k by the appearance of smaller graupel particles below the freezing level. The enhanced rain amount in the semicontinental cloud that is shown in Figure 9c as compared to Figure 9a is therefore a result of the contributions of both water drops and graupel particles. Very large graupel particles (about 1 cm diameter) appear after 46 min (Figure 10k); however, their concentrations are extremely low (about 1 m^{-3}).

[56] The early rain development in the semicontinental cloud also affects the vertical wind. Figure 11 presents the vertical wind velocities at 46 min in the two cloud types. Comparing the vertical wind velocities in the reference cases (cases 1 and 5, Figures 11b and 11a) shows that at 46 min the downdraft in the semicontinental cloud is very strong around the cloud's center (maximum of about $-5.$ m s^{-1}) extending from the surface up to about 2.5 km height. In the continental cloud there is still updraft near the center (maximum of 4.5 m s^{-1}) extending up to about 5 km, with much smaller downdrafts (less than about -0.5 m s^{-1}) between the heights of 1 to 5 km.

[57] Since it was already demonstrated above that the effects of the GCCN on the maritime cloud is minimal, we will concentrate now on the effects of the combined GCCN and enhanced IN (case 4 in Table 2) on the development of the continental cloud and the formation of rain in it. This is done by comparing case 4 with the reference case (case 1). Figure 12 presents the number distributions of the different hydrometeors at the center of the cloud as a function of height after 26 and 46 min from the start of the simulation. Figure 12 also displays the volume distributions from case 4. It becomes clear that the effect of the GCCN is to enhance the development of the large drops [see also *Johnson*, 1982; *Cooper et al.*, 1997; *Yin et al.*, 2000], leading to enhanced growth by collection and rapid development of the rain on the ground (seen best in Figures 12l and 12r). What is also shown on Figure 12 is that the graupel particles grow rapidly because of enhanced riming resulting from the higher collection efficiency of the larger cloud drops (compare Figures 12h and 12g and Figures 12q

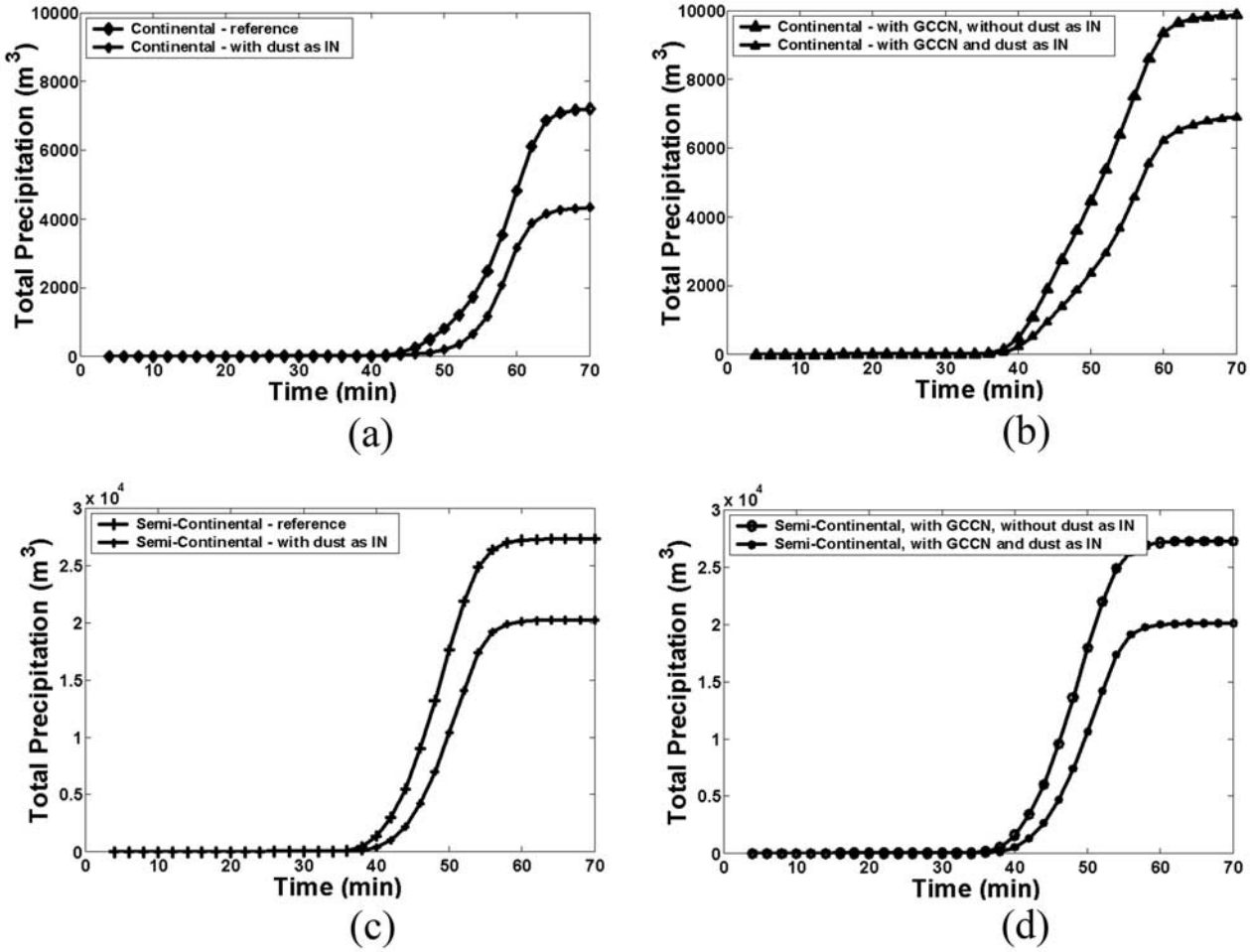

Figure 9. Comparison of total precipitation (in m^3) that fell from a cloud with the initial condition shown in Table 2.

and 12p). It should be pointed out that the growth of graupel particles shown on Figure 12 when both GCCN and enhanced IN are included, is slower than in the case when only GCCN are present (not shown here). This is because in Figure 12 many of the droplets that are the source of riming for the graupel particles' growth are nucleated to form ice crystals because of the increase in IN concentrations.

[58] As the graupel particles descend below the freezing level, shedding of drops from the water layers around the melting graupel particles takes place (see *Yin et al.* [2000] for details). The water drops that are thrown off reduce the size of the graupel particles (Figures 12p and 12q) and are added to the raindrops, as can be seen at the lower levels in Figures 12k and 12l.

[59] The ice crystal's concentrations in the cloud increase because of the added dust as IN (see Figures 12e and 12f). However, most of the ice crystals remain smaller and are found at higher levels (compare Figures 12n and 12m). The growth of the ice crystals is reduced because of the more effective depletion by riming of the larger water drops and because of the competition for the available water vapor by the increased number of ice crystals. Owing to their small size most of these ice crystals do not precipitate; they remain at the higher levels and are advected to the side of the cloud to form a wider cloud (see Table 3 and Figure 14b, to be discussed later). The advection of the ice crystals to the side of the cloud leads to a reduced total rainfall on the ground, as seen in Figure 9b.

[60] The effects described above also influence the vertical velocities in the cloud. Figures 11c and 11d show that the increased graupel number and size due to enhanced freezing and riming, respectively, results in heavier mass loading, leading to more wide spread downdrafts and weaker and narrower updrafts as compared to the reference cases (Figures 11a and 11b). In contrast, the enhanced ice crystal concentrations and the enhanced growth of the graupel particles lead to enhanced release of latent heat during riming and to a small increase in the updrafts near cloud center (compare Figure 11d with maximum updraft of about 4.5 m s^{-1} to 4.3 m s^{-1} in Figure 11b). This small increase in updraft does not change the cloud depth but lifts more drops and ice crystals closer to cloud top. These particles could then be advected sideways by the horizontal winds.

4.2.3. Effect on the Height and Horizontal Extent of the Clouds

[61] Cloud top height and cloud width may have a large impact on the assessment of the cloud contribution to the

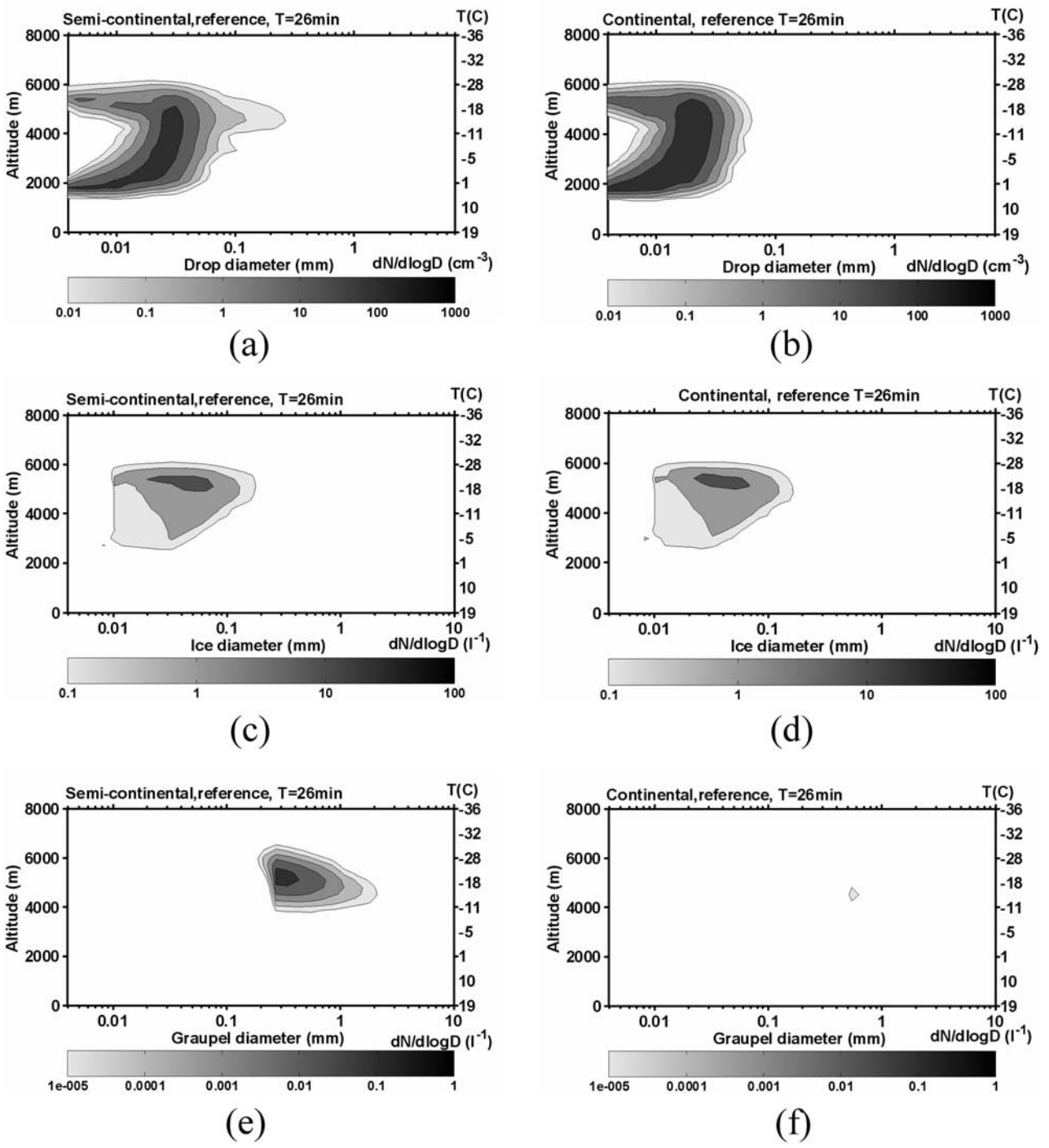

Figure 10. Comparison of the number size distributions of water drops, ice crystals, and graupel particles at cloud center between the reference (left) semicontinental and the (right) continental clouds (cases 1 and 5 in Table 2) after 26 and 46 min.

radiative balance of the atmosphere [*Lohmann and Feichter*, 2005]. Although satellites are being used now to estimate the effects of aerosols on the morphology of clouds [*Kaufman et al.*, 2005; *Koren et al.*, 2005], it is very difficult to separate the effects of the aerosols from the effects of the larger-scale meteorology (e.g., temperature and humidity profiles, wind shear, etc.). The use of numerical models provides a way to separate these effects and at least obtain a qualitative picture of the possible influence of the aerosols on the morphology of the clouds. It is not the main intention of this paper to discuss this relative effect in detail, but preliminary conclusions may be inferred from the results shown here. For this purpose, the maximum height and horizontal width of the clouds at the time of maximum rainfall rate were calculated, and they are presented in Table 3. To illustrate this further, Figures 13 and 14 show the spatial

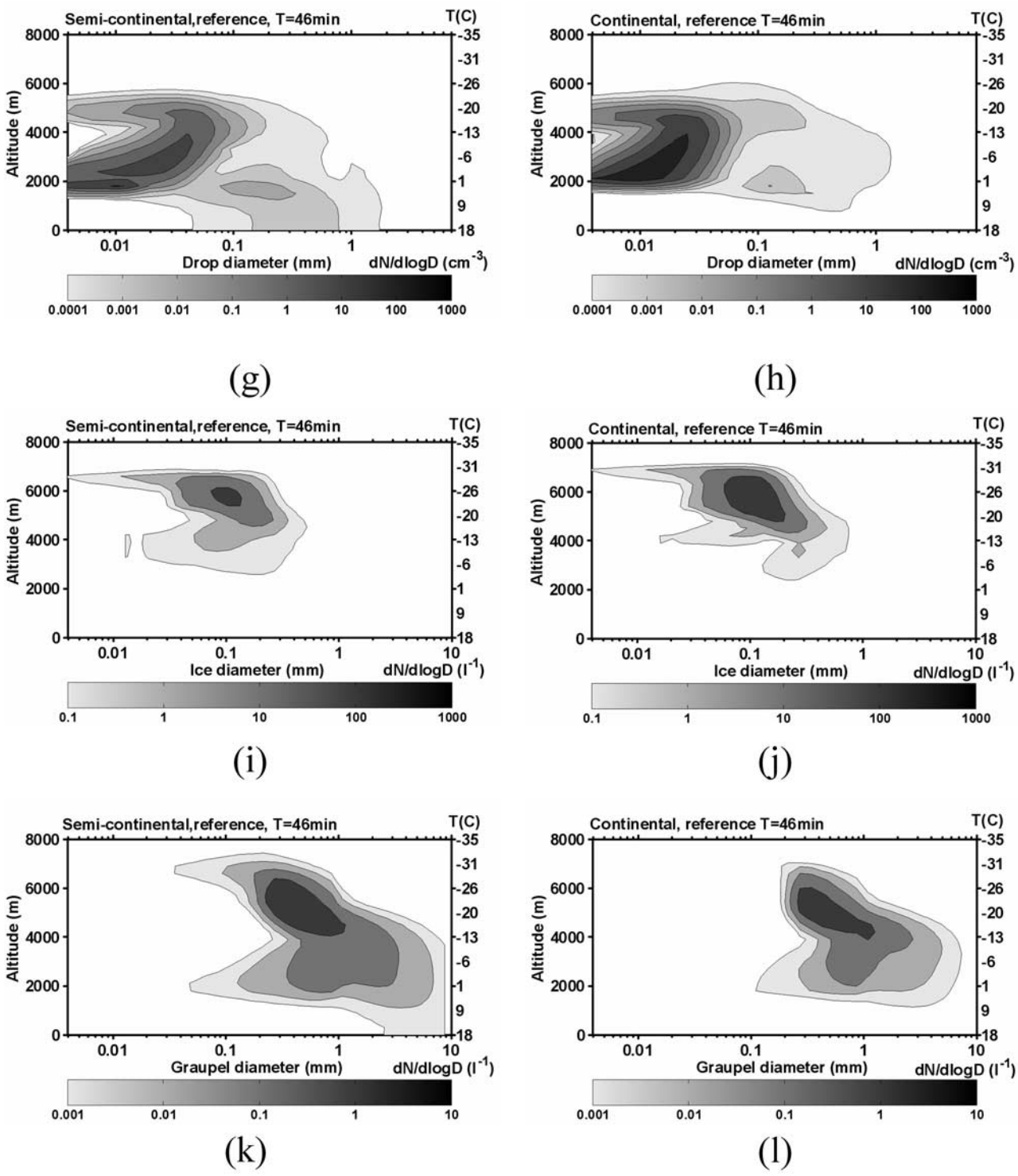

Figure 10. (continued)

distribution of the mixing ratio of water, ice and graupel at the time of maximum rainfall on the ground.

[62] Figure 13 presents contours of the mixing ratios in the reference clouds (cases 1 and 5 in Table 2). It shows that for the temperature profiles used in this study (corresponding to a typical winter time conditions over the eastern Mediterranean Sea), increases in CCN from about 300 cm^{-3}, corresponding to clean maritime (or semicontinental) clouds to about 900 cm^{-3} corresponding to more polluted continental clouds lead to increases of about 900 m in cloud height. Although the total mass of ice at the upper portions of the continental cloud is higher than in the semicontinental case, the width of the two clouds is similar (see Table 3 and Figure 13).

[63] A comparison of the changes in height and width of the clouds affected by GCCN and enhanced IN reveals that their effects on the continental clouds are stronger than on the maritime one. Table 3 and Figure 14 show that the width

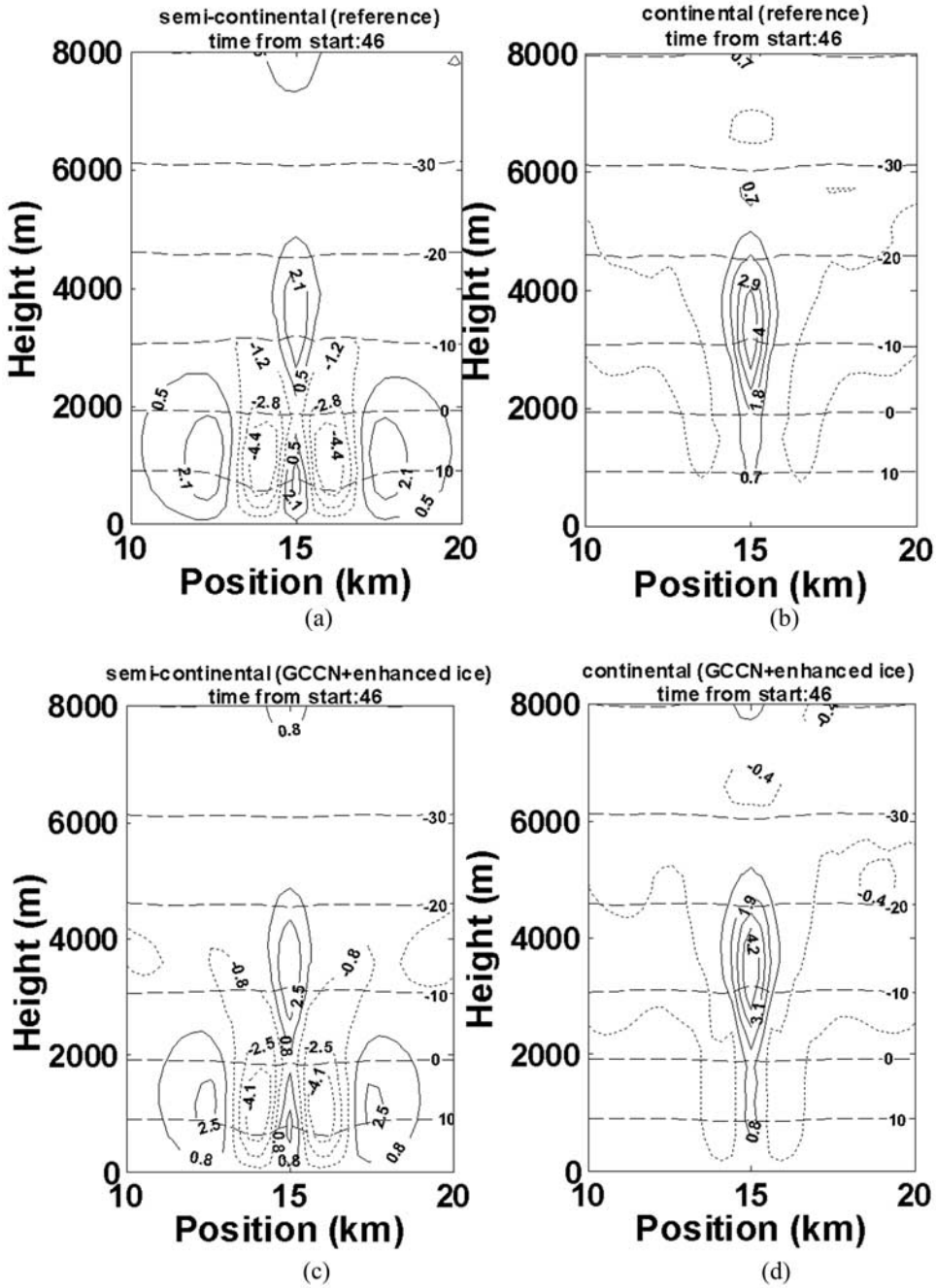

Figure 11. The vertical velocities in the reference (a) semicontinental and (b) continental clouds (cases 5 and 1, respectively, in Table 2) and the clouds affected by giant cloud condensation nuclei (GCCN) and enhanced ice nuclei IN (cases 4 and 8) after 46 min.

of the affected continental cloud increases by 600 m, whereas the width of the semicontinental cloud is not affected. The height of the continental cloud changes very little, although a very small decrease is seen in Figure 14. This slight decrease could be a result of the heavier mass loading due to the larger mass of graupel and larger mass of the ice crystals. The higher ice mass at the upper reaches of both case 1 and case 4 (in Table 2) suggests that in the presence of wind shear, the horizontal spread of the more polluted continental cloud will be larger, forming a larger anvil. Considering this effect in a cloud field as viewed from satellites, it would mean a higher cloud fraction with stronger effects on the radiation field.

[64] Figures 13 and 14 also demonstrate the effect of the GCCN on the spread of rainfall on the ground. In Figures 13 and 14 we see that the rain is mainly falling around the center of the updraft. In the continental clouds the drops are smaller and the only hydrometeors that manage to grow to large sizes are those that are very close to the updrafts. Smaller hydrometeors are pushed sideways and many of them never manage to fall down as rain. This leads to a more narrow precipitation region. In the semicontinental

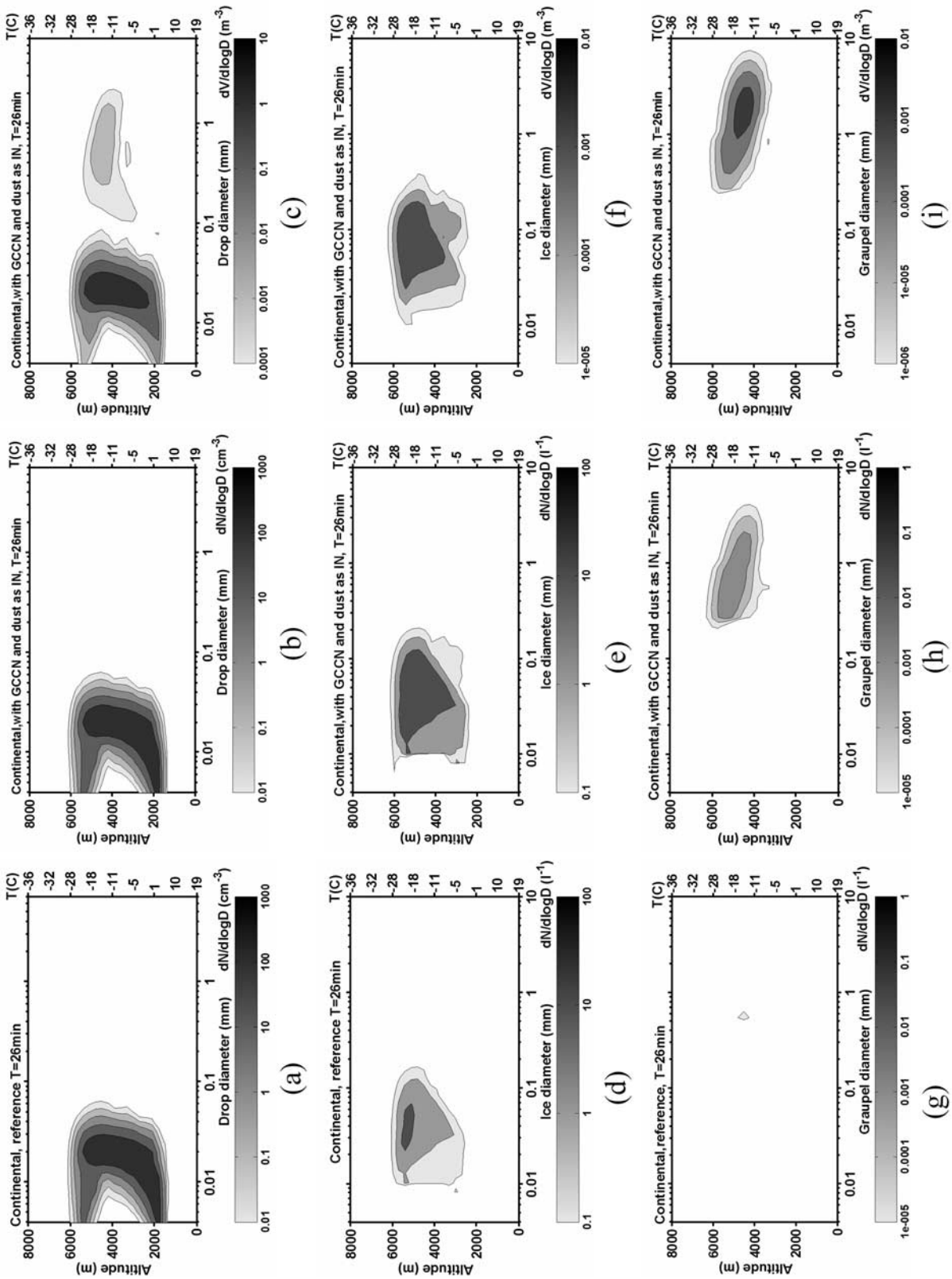

Figure 12. Comparison of the hydrometeors size distribution at the center of the continental cloud between the reference case (case 1) and the case with both GCCN and enhanced IN (case 4), after 26 and 46 min. The right plot in each row shows the hydrometeor volume distributions of case 4.

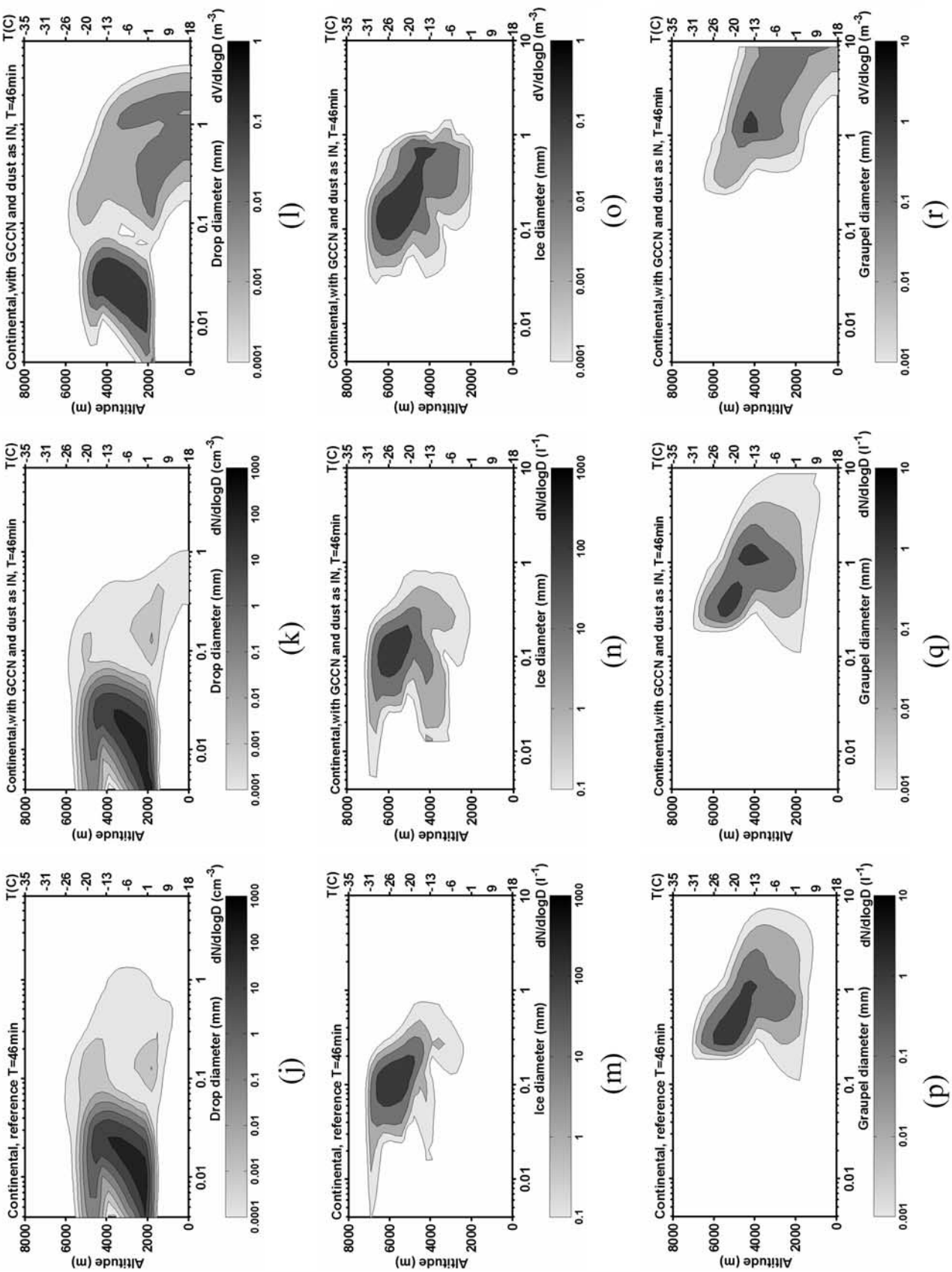

Figure 12. (contnued)

Table 3. Maximum Heights and Widths of the Reference Clouds and Those of the Clouds Affected by GCCN Plus Enhanced Ice Production[a]

Scenario	Time of Maximum Rain Rate		
	Time, min	Cloud Top, m	Cloud Width, m
1 continental reference	62	6600	6900
4 continental with GCCN and dust as IN	58	6300	7500
5 semicontinental reference	52	5700	6900
8 semicontinental with GCCN and dust as IN	54	5700	6900

[a]The maximum size is determined by the contours of 0.3 g kg^{-1}.

clouds the hydrometeors are larger and even those that are advected sideways are large enough to fall as rain. This results in a wider area of precipitation. These differences are seen in the size of the ''neck'' that appears in Figures 13 and 14. In other words, under the same meteorological conditions, the maritime clouds will initiate rain earlier, produce more rain, and spread it over a larger area than the continental clouds. The results also demonstrate that the late start and the shorter duration of rain from the continental clouds implies a lower rain efficiency, a larger fraction of water that still remains in the atmosphere after the rain, a longer-lived clouds and an efficient redistribution of water vapor in the troposphere from the lower to the upper levels.

5. Summary and Conclusions

[65] This paper describes the chemical and physical characteristics of aerosols measured during a dust storm that passed over the eastern Mediterranean region on 28 January 2003. It also uses these findings in order to investigate the possible role that mineral dust particles coated with sea salt could have in modifying the development of clouds and precipitation. The measured vertical profile of aerosol properties showed that large concentrations of coarse particles (>1 μm) were present up to an altitude of 2.5 km above msl. The chemical analyses of individual particles revealed that a large fraction of the particles were composed of internal mixtures of mineral dust and sea salt (~35% in the coarse mode). The presence of soluble material such as sulfate over the Mediterranean [*Levin et al.*, 1996] and over China [*Trochkine et al.*, 2003] or sea salt (as was found in this study) on dust particles enhances CCN concentration and affects the production of rain.

[66] In the present study we used the measured size distribution and the chemical composition of the aerosols as initial conditions for simulating cloud development using the Tel Aviv University 2D cloud model. The results show that rain falling from the more maritime clouds started earlier, produced larger amount, and covered a wider area than that from the continental clouds.

[67] On the other hand, the lifetime of the continental clouds, having higher concentrations of droplets, was longer than the more maritime clouds. Continental clouds also grew to higher levels than maritime clouds.

[68] Our results also show that ignoring the ice nucleating (IN) ability of the mineral dust, but allowing the soluble component to act as efficient GCCN, enhances the growth of drops and graupel particles in continental clouds by collection and riming, respectively. In these simulations, the rain amounts in the continental clouds increased by as much as 37% compared to those without the coarse-mode CCN. On the other hand, if the properties of dust particles as efficient IN are also included, the rain amount is reduced.

[69] It is also shown that introducing similar particles into the more maritime clouds does not produce any significant

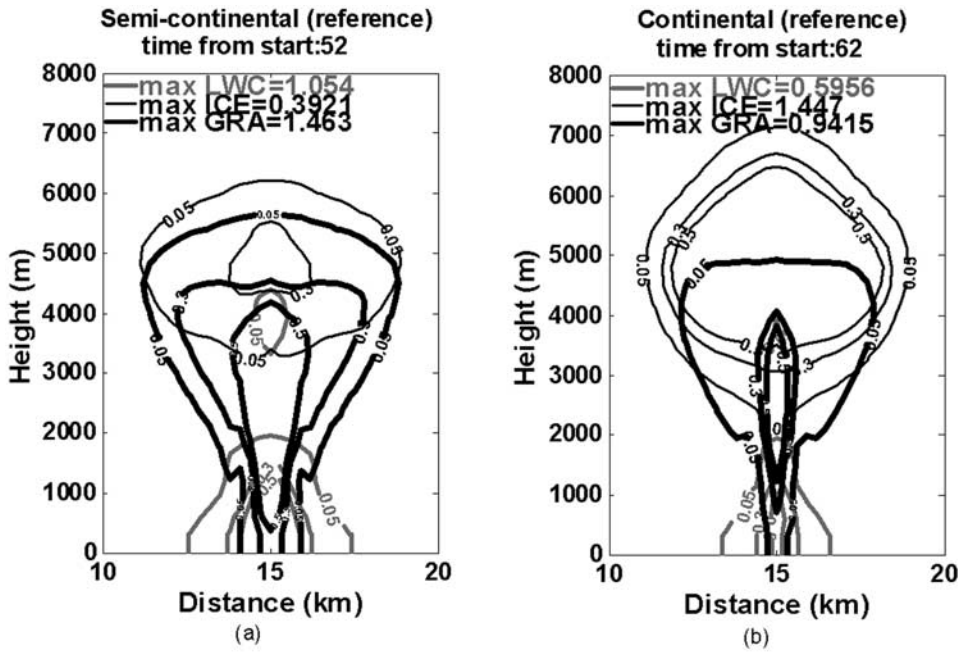

Figure 13. Distribution of water, ice, and graupel particles mass content in g kg^{-1} in the reference continental and semicontinental clouds at the time of maximum precipitation on the ground.

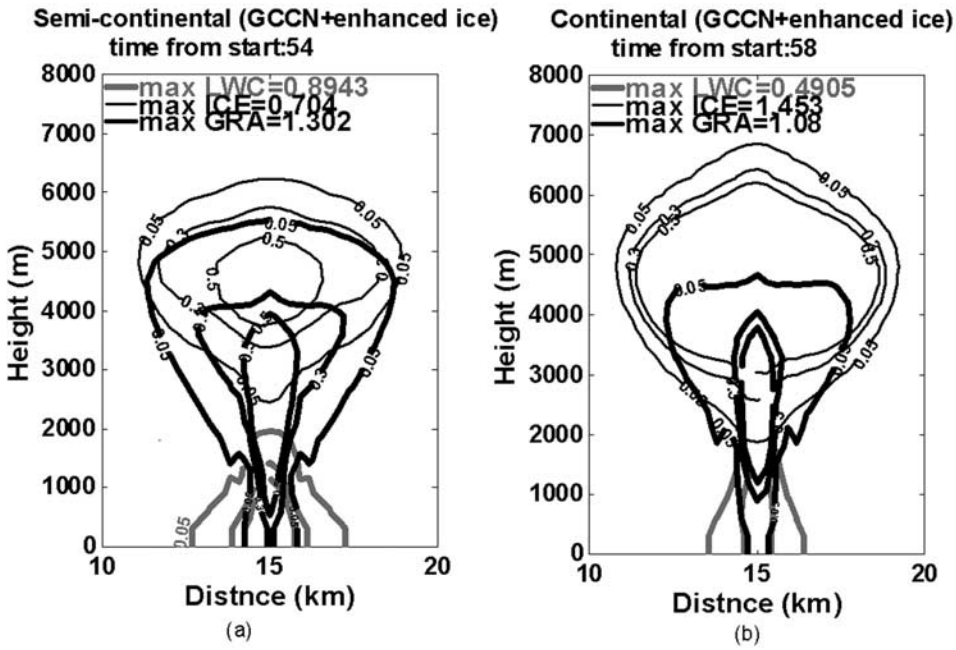

Figure 14. As in Figure 13 except for continental and semicontinental clouds affected by GCCN and by enhanced IN at the time of maximum precipitation on the ground.

changes in the cloud development and in the rain amount on the ground. Furthermore, GCCN together with enhanced IN affect the horizontal dimensions of the continental clouds by increasing it by as much as 9% in our simulation. On the other hand, the same combination of particles slightly reduces the height of the continental clouds (primarily because of the enhanced mass of the drops and graupel) and has little effect on the maritime clouds. Of course, superimposing these results on more realistic conditions with wind shear would considerably increase the horizontal spread, thus increasing cloud fraction as seen from space.

[70] **Acknowledgments.** This paper is part of the research carried out in the MEIDEX and is dedicated to the memory of the seven astronauts of the space shuttle Columbia in mission STS-107: Rick Husband, William McCool, Michael Anderson, Laurel Clark, David Brown, Kalpana Chawla, and Ilan Ramon. MEIDEX is a joint project of the Israel Space Agency and NASA. It was partly funded by the Israeli Ministry of Science under the MEIDEX project and by the United States-Israel Binational Science Foundation (grant 2000308). We thank David Shtivelman from Tel Aviv University for assisting with the instruments. Part of the work on this paper was carried out by Z.L. during his sabbatical leave at UMBC-GEST, NASA Goddard Space Flight Center.

References

Al-Momani, I. F., S. Tuncel, Ü. Eler, E. Ördel, G. Sirin, and G. Tuncel (1995), Major ion composition of wet and dry deposition in the eastern Mediterranean basin, *Sci. Total Environ.*, *164*, 75–85.

Alpert, P., and E. Ganor (1993), A jet-stream associated heavy dust storm in the western Mediterranean, *J. Geophys. Res.*, *98*, 7339–7349.

Andreae, T. W., M. O. Andreae, C. Ichoku, W. Maenhaut, J. Cafmeyer, A. Karnieli, and L. Orlovsky (2002), Light scattering by dust and anthropogenic aerosol at a remote site in the Negev desert, Israel, *J. Geophys. Res.*, *107*(D1), 4008, doi:10.1029/2001JD900252.

Borys, R. D., D. H. Lowenthal, S. A. Cohn, and W. O. J. Brown (2003), Mountaintop and radar measurements of anthropogenic aerosol effects on snow growth and snowfall rate, *Geophys. Res. Lett.*, *30*(10), 1538, doi:10.1029/2002GL016855.

Cooper, W. A., R. T. Bruintjes, and G. K. Mather (1997), Some calculations pertaining to hygroscopic seeding with flares, *J. Appl. Meteorol.*, *36*, 1449–1469.

DeMott, P. J., K. Sassen, M. R. Poellet, D. Baumgardner, D. C. Rogers, S. D. Brooks, A. J. Prenni, and S. M. Kreidenweis (2003), *Geophys. Res. Lett.*, *30*(14), 1732, doi:10.1029/2003GL017410.

di Sarra, A., T. Di Iorio, M. Cacciani, G. Fiocco, and D. Fuà (2001), Saharan dust profiles measured by lidar at Lampedusa, *J. Geophys. Res.*, *106*, 10,335–10,348.

Falkovich, A. H., E. Ganor, Z. Levin, P. Formenti, and Y. Rudich (2001), Chemical and mineralogical analysis of individual mineral dust particles, *J. Geophys. Res.*, *106*, 18,029–18,036.

Feingold, G., W. R. Cotton, S. M. Kreidenweis, and J. T. Davis (1999), The impact of giant cloud condensation nuclei on drizzle formation in stratocumulus: Implications for cloud radiative properties, *J. Atmos. Sci.*, *56*, 4100–4117.

Ganor, E. (1994), The frequency of Saharan dust episodes over Tel Aviv, Israel, *Atmos. Environ.*, *28*, 2867–2871.

Ganor, E., and H. Foner (1996), The mineralogical and chemical properties and behavior of Aeolian Saharan dust over Israel, in *The Impact of Desert Dust Across the Mediterranean (1996)*, edited by S. Guerzoni and R. Chester, pp. 163–172, Springer, New York.

Ganor, E., and Y. Mamane (1982), Transport of Saharan dust across the eastern Mediterranean, *Atmos. Environ.*, *16*, 581–587.

Ganor, E., Z. Levin, and R. Van Grieken (1998), Composition of individual aerosol particles above the Israeli Mediterranean coast during the summer time, *Atmos. Environ.*, *32*, 1631–1642.

Ganor, E., H. A. Foner, H. G. Bingemer, R. Udiste, and I. Setter (2000), Biogenic sulfate generation in the Mediterranean Sea and its contribution to the sulfate anomaly in the aerosol over Israel and eastern Mediterranean, *Atmos. Environ.*, *34*, 3453–3462.

Givati, A., and D. Rosenfeld (2004), Quantifying precipitation suppression due to air pollution, *J. Appl. Meteorol.*, *43*, 1038–1056.

Grosch, M., and H.-W. Georgii (1976), Elemental composition of atmospheric aerosols and natural ice forming nuclei, *J. Rech. Atmos.*, *10*, 227–232.

Hallett, J., and S. C. Mossop (1974), Production of secondary ice crystals during the riming process, *Nature*, *249*, 26–28.

Israelevich, P. L., E. Ganor, Z. Levin, and J. H. Joseph (2003), Annual variations of physical properties of desert dust over Israel, *J. Geophys. Res.*, *108*(D13), 4381, doi:10.1029/2002JD003163.

Johnson, D. B. (1982), The role of giant and ultragiant aerosol particles in warm rain initiation, *J. Atmos. Sci.*, *39*, 448–460.

Kaufman, Y. J., I. Koren, L. A. Remer, D. Rosenfeld, and Y. Rudich (2005), The effect of smoke, dust and pollution aerosol on shallow cloud development over the Atlantic Ocean, *Proc. Natl. Acad. Sci. U. S. A.*, *102*, 11,207–11,212.

Khain, A., and A. Pokrovsky (2004), Simulation of effects of atmospheric aerosols on deep turbulent convective clouds using a spectral microphysics

mixed-phase cumulus cloud model. Part II: Sensitivity study, *J. Atmos. Sci.*, *61*, 2983–3001.

Koren, I., Y. J. Kaufman, D. Rosenfeld, L. A. Remer, and Y. Rudich (2005), Aerosol invigoration and restructuring of Atlantic convective clouds, *Geophys. Res. Lett.*, *32*, L14828, doi:10.1029/2005GL023187.

Kouimtzis, T., and C. Samara (1995), *Airborne Particulate Matter*, 339 pp., Springer, New York.

Kubilay, N., M. Kocak, T. Cokacar, T. Oguz, G. Kouvarakis, and N. Mihalopoulos (2002), Influence of Black Sea and local biogenic activity on the seasonal variation of aerosol sulfur species in the eastern Mediterranean atmosphere, *Global Biogeochem. Cycles*, *16*(4), 1079, doi:10.1029/2002GB001880.

Levin, Z., and J. D. Lindberg (1979), Size distribution, chemical composition, and optical properties of urban and desert aerosols in Israel, *J. Geophys. Res.*, *84*, 6941–6950.

Levin, Z., E. Ganor, and V. Gladstein (1996), The effects of desert particles coated with sulfate on rain formation in the eastern Mediterranean, *J. Appl. Meteorol.*, *35*, 1511–1523.

Lohmann, U., and J. Feichter (2005), Global indirect aerosol effects: A review, *Atmos. Chem. Phys.*, *5*, 715–737.

Low, T. B., and R. List (1982a), Collision, coalescence and breakup of raindrops: Part I. Experimentally established coalescence efficiencies and fragment size distribution in breakup, *J. Atmos. Sci.*, *39*, 1591–1606.

Low, T. B., and R. List (1982b), Collision, coalescence and breakup of raindrops: Part II. Parameterization of fragment size distributions, *J. Atmos. Sci.*, *39*, 1607–1618.

Luria, M., M. Peleg, G. Sharf, D. Siman Tov-Alper, N. Spitz, Y. Ben Ami, Z. Gawii, B. Lifschitz, A. Yitzchaki, and I. Seter (1996), Atmospheric sulfur over the Mediterranean region, *J. Geophys. Res.*, *101*, 25,917–25,930.

Mahowald, N., and L. Kiehl (2003), Mineral aerosol and cloud interactions, *Geophys. Res. Lett.*, *30*(9), 1475, doi:10.1029/2002GL016762.

Meyers, M. P., P. J. DeMott, and W. R. Cotton (1992), New primary ice-nucleation parameterizations in an explicit cloud model, *J. Appl. Meteorol.*, *31*, 708–721.

Mihalopoulos, N., E. Stephanou, M. Kanakidou, S. Pilitsidis, and P. Bousquet (1997), Tropospheric aerosol ionic composition in the eastern Mediterranean region, *Tellus, Ser. B*, *49*, 314–326.

Pardess, D., Z. Levin, and E. Ganor (1992), A new method for measuring the mass of sulfur in single aerosols particles, *Atmos. Environ., Part A*, *26*, 679–680.

Pruppacher, H. R., and J. D. Klett (1997), *Microphysics of Clouds and Precipitation*, 1954 pp., Springer, New York.

Reisin, T., Y. Yin, Z. Levin, and S. Tzivion (1998), Development of giant drops and high reflectivity cores in Hawaiian clouds: Numerical simulation using a kinematic model with detailed microphysics, *Atmos. Res.*, *45*, 275–297.

Rosenfeld, D., Y. Rudich, and R. Lahav (2001), Desert dust suppressing precipitation: A possible desertification feedback loop, *Proc. Natl. Acad. Sci. U. S. A.*, *98*, 5975–5980.

Trochkine, D., Y. Iwasaka, A. Matsuki, M. Yamada, Y.-S. Kim, T. Nagatani, D. Zhang, G.-Y. Shi, and Z. Shen (2003), Mineral aerosol particles collected in Dunhuang, China, and their comparison with chemically modified particles collected over Japan, *J. Geophys. Res.*, *108*(D23), 8642, doi:10.1029/2002JD003268.

Tzivion, S., G. Feingold, and Z. Levin (1987), An efficient numerical solution to the stochastic collection equation, *J. Atmos. Sci.*, *44*, 3139–3149.

van den Heever, S. C., G. G. Carrio, W. R. Cotton, P. J. DeMott, and A. J. Prenni (2005), Impacts of nucleating aerosol on Florida convection. Part I: Mesoscale simulations, *J. Atmos. Sci.*, in press.

Wanger, A., et al. (2000), Long-range transport of air pollutants over the eastern Mediterranean: Measurements, model simulations, and synoptic analyses, *J. Geophys. Res.*, *105*, 7177–7186.

Wurzler, S., T. G. Reisin, and Z. Levin (2000), Modification of mineral dust particles by cloud processing and subsequent effects on drop size distributions, *J. Geophys. Res.*, *105*, 4501–4512.

Yin, Y., Z. Levin, T. G. Reisin, and S. Tzivion (2000), The effect of giant cloud condensation nuclei on the development of precipitation in convective clouds—A numerical study, *Atmos. Res.*, *53*, 91–116.

Yin, Y., S. Wurzler, Z. Levin, T. G. Reisin, and S. Tzivion (2002), Interactions of mineral dust particles and clouds: Effects on precipitation and cloud optical properties, *J. Geophys. Res.*, *107*(D23), 4724, doi:10.1029/2001JD001544.

E. Ganor, Z. Levin, and A. Teller, Department of Geophysics and Planetary Sciences, Tel Aviv University, 69989 Ramat Aviv, Tel Aviv, Israel. (zev@hail.tau.ac.il)

Y. Yin, Institute of Mathematical and Physical Sciences, University of Wales Aberystwyth, SY23 3BZ, Aberystwyth, UK.